

Counter Terms for Low Momentum Nucleon-Nucleon Interactions

Jason D. Holt¹, T.T.S. Kuo¹, G.E. Brown¹ and Scott K. Bogner²¹Department of Physics, State University of New York at Stony Brook Stony Brook, New York 11794²Institute for Nuclear Theory, Univ. of Washington, Seattle, WA 98195

(Dated: February 9, 2020)

There is much current interest in treating low energy nuclear physics using the renormalization group (RG) and effective field theory (EFT). Inspired by this RG-EFT approach, we study a low-momentum nucleon-nucleon (NN) interaction, $V_{low\ k}$, obtained by integrating out the fast modes down to the scale 2fm^{-1} . Since NN experiments can only determine the effective interaction in this low-momentum region, our chief purpose is to find such an interaction for complex nuclei whose typical momenta lie below this scale. In this paper we find that $V_{low\ k}$ can be satisfactorily accounted for by the counter terms suggested by the RG-EFT approach. The coefficients, C_n , for the counter terms of the form $C_n k^n$ ($n=0,2,4,\dots$) have been accurately determined, and results derived from several meson-exchange NN interaction models are compared. Finally we discuss the use of these methods for computing shell model matrix elements and compare the results using $V_{low\ k}$ to those obtained with the Sussex interaction.

PACS numbers: 21.60.Cs; 21.30.Fe; 27.80.+j

I. INTRODUCTION

Since the pioneering work of Weinberg [1], there has been much progress and interest in treating low-energy nuclear physics using the renormalization group (RG) and effective field theory (EFT) approach [2, 3, 4, 5, 6, 7]. A central idea here is that physics in the infrared region must be insensitive to the details of the short range (high momentum) dynamics. In low-energy nuclear physics, we are probing nuclear systems with low-energy probes of wave length λ ; such probes cannot reveal the short range details at distances much smaller than λ . Furthermore, our understanding about the short range dynamics is still preliminary, and model dependent. Because of these considerations, a central step in the RG-EFT approach is to divide the fields into two categories: slow fields and fast fields, separated by a chiral symmetry breaking scale 1GeV . Then by integrating out the fast fields, one obtains an effective field theory for the slow fields only. This approach has been very successful in treating low-energy nuclear systems, as discussed in the references cited above. In order to have an effective interaction appropriate for complex nuclei in which typical nucleon momenta are $< k_F$, we separate fast and slow modes by a scale much smaller than k_F , namely 2fm^{-1} . In fact nucleon-nucleon experiments give a unique effective interaction only up to this scale.

This RG-EFT idea has been employed recently by several authors [8, 9, 10, 11, 12] in a new development for the nucleon-nucleon (NN) interaction: the derivation of a low-momentum NN potential $V_{low\ k}$ using renormalization group decimation methods. There are a number of realistic models [14, 15, 16, 17, 18] for the nucleon-nucleon (NN) potential V_{NN} . While these models agree

well in the low momentum (long range) region, where they are just given by the one pion exchange interaction, in the high momentum (short range) region they are rather uncertain and, in fact, differ significantly from one another. Thus it would be desirable to remove these uncertainties and model dependence from the high momentum components of the various model NN potentials. Following the RG-EFT idea to achieve this end, it would seem to be appropriate to integrate out the high momentum modes of the various V_{NN} models. This is how the $V_{low\ k}$ was derived, and in section II, we provide a brief outline of the derivation based on T-matrix equivalence.

The low-momentum NN potential, $V_{low\ k}$, reproduces the deuteron binding energy, low-energy NN phase shifts and the low-momentum half-on-shell T-matrix. Furthermore, it is a smooth potential and can be used directly in nuclear many body calculations, avoiding the calculation of the Brueckner G-matrix [8, 9, 10, 11, 12]. At the present, no algebraic form exists for $V_{low\ k}$, and in the present work we study the feasibility of finding such an expression.

A central result of modern renormalization theory is that a general RG decimation generates an infinite series of counter terms [2, 4] consistent with the input interaction. When we derive our low momentum interaction, the high momentum modes of the input interaction are integrated out. Does this decimation also generate a series of counter terms? If so, then what are the counter terms so generated? We study these questions in section III where we carry out an accurate determination of the counter terms and show that this approach reproduces not only $V_{low\ k}$, but the deuteron binding energy and low-energy phase shifts as well. Finally in section IV, we

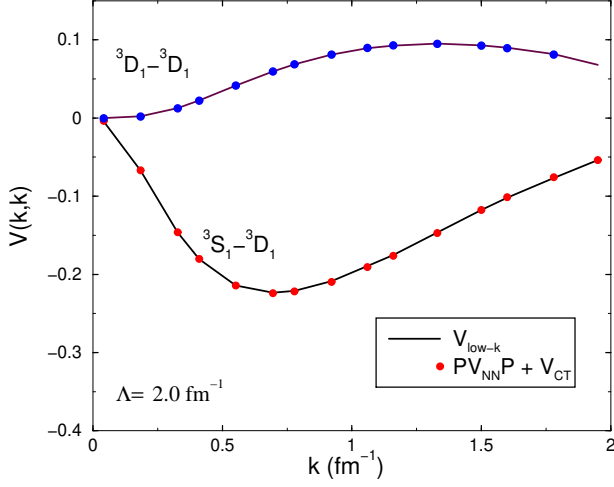


FIG. 2: Comparison of $V_{\text{low } k}$ with $P V_{\text{NN}} P$ plus counter terms, for 3S_1 - 3D_1 and 3D_1 channels.

If we take the projection operator P to project onto states with momentum less than Λ , namely $P = \int_{k < \Lambda} d^3k |k\rangle \langle k|$, we can rewrite V_{bare} of Eq.(5) as $P V_{\text{bare}} P$. From now on we shall also abbreviate V_{counter} as V_{CT} . The above counter term approach for $V_{\text{low } k}$ is similar to that used in RG-EFT [2, 4], as both methods impose some momentum cutoff, integrate out the high momentum modes, and then attempt to recover the information contained in those states in a counter term series. The main difference, however, is the potential to which V_{CT} is added. As already noted, in the representation of $V_{\text{low } k}$ given above, we begin with a bare NN potential projected onto the low momentum states. In the RG-EFT model, the counter terms are added to V_{light} , which is given by light mesons below the cutoff scale. So, V_{light} is obtained by integrating out heavy mesons above the cutoff scale, and is usually taken to be $V_{\text{one pion}}$.

The counter term coefficients are determined using standard fitting techniques so that the right hand side of Eq.(5) provides a best fit to the left hand side of the same equation. We perform this fitting over all partial wave channels, and find consistently good agreement. In Fig. 1 we compare some 1S_0 and 3S_1 matrix elements of $(P V_{\text{bare}} P + V_{\text{CT}})$ with those of $V_{\text{low } k}$ for momenta below the cutoff. A similar comparison for the 3S_1 - 3D_1 and 3D_1 channels is displayed in Fig. 2. As these figures show, the two methods yield nearly identical effective interactions. Moreover, the V_{eff} obtained from this counter term approach can be seen to preserve phase shifts. We show this result in Fig. 3, where the phase shifts are plotted up to a lab energy of 325 MeV, and only at this high momentum, do they begin to differ slightly from those obtained from $V_{\text{low } k}$. In passing, we mention

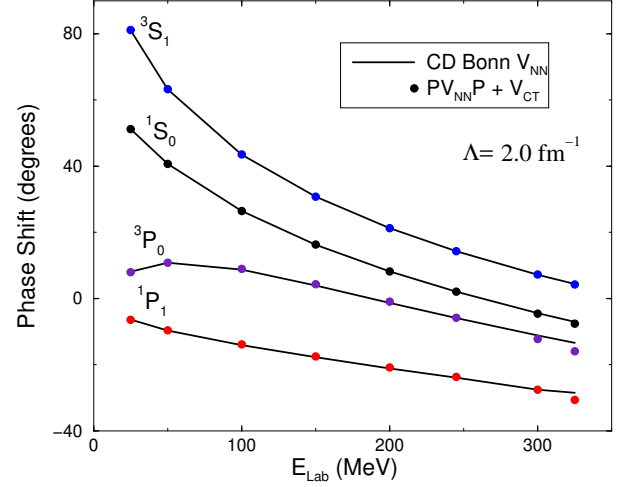


FIG. 3: Comparison of phase shifts given by V_{NN} and $P V_{\text{NN}} P$ plus counter terms.

that the deuteron binding energy is also accurately reproduced by our counter term approach. To illustrate, for the CD Bonn potential the deuteron binding energy given by the full potential and the counter term approach are respectively 2.225 and 2.224 MeV. Clearly, we can very accurately reproduce $V_{\text{low } k}$ and all its results by using $P V_{\text{bare}} P + V_{\text{CT}}$.

We note that in the present work the counter term coefficients are determined from the Hermitian $V_{\text{low } k}$, which is obtained by performing an Okubo transformation mentioned earlier. We have verified that the deuteron binding energy and low-energy phase shifts are also preserved by the Hermitian $V_{\text{low } k}$. Since the non-Hermiticity of the ALS interaction is very slight, the counter terms obtained for these two interactions have been found to be quite similar to each other.

Now let us examine the counter terms themselves. In Table I, we list some of the counter term coefficients, using CD Bonn as our bare potential. In the table we list only the counter terms for the 1S_0 and 3S_1 - 3D_1 partial waves; we have found that the counter terms for all the other waves are much smaller. (A complete table of counter terms for all the partial waves is given in Table V.) This tells us an interesting result, namely, except for the above two channels, $V_{\text{low } k}$ is very similar to $P V_{\text{bare}} P$ alone. It may be noted that the coefficients C_2 and C_2^0 are generally different for cross channels (such as 3S_1 - 3D_1); this is due to the fact that the matrix elements $\langle {}^3S_1; k | \mathcal{V}_{\text{low } k} | {}^3D_1; k^0 \rangle$ and $\langle {}^3S_1; k^0 | \mathcal{V}_{\text{low } k} | {}^3D_1; k \rangle$ are generally different. We also point out that the coefficients C_6 are found to be very small, indicating that the above power series expansion converges rapidly. In the last row of the table, we list the rms deviations be-

TABLE I: Coefficients of the counter terms for $V_{\text{low } k}$ obtained from the CD-Bonn potential using $\Lambda = 2 \text{ fm}^{-1}$. The unit for the combined quantity $C_n k^n$ is fm , with momentum k in units of fm^{-1} .

	1S_0	3S_1	3S_1	3D_1	3D_1
C_0	-0.1580	-0.4646	0	0	
C_2	-0.0131	0.0581	-0.0017	-0.0005	
C_2^0	-0.0131	0.0581	0.0301	-0.0005	
C_4	0.0004	-0.0011	-0.0013	0.0006	
C_4^0	-0.0011	-0.0113	-0.0047	-0.0018	
C_6	-0.0004	-0.0004	0.0006	-0.0001	
C_6^0	-0.0005	0.0005	-0.0001	-0.0001	
C_6^{00}	-0.0005	0.0005	-0.0003	-0.0001	
terms	0.0002	0.0003	0.0028	0.0003	

TABLE II: Comparison of counter terms for $V_{\text{low } k}$ obtained from the CD-Bonn, Nijmegen and Paris potentials using $\Lambda = 2 \text{ fm}^{-1}$. The units for the counter coefficients are the same as in Table I.

	C_0	C_2	C_2^0	
1S_0	-0.158	-0.0131	-0.0131	CD-Bonn
	-0.570	0.0111	0.0111	Argonne V18
	-0.753	-0.0099	-0.0099	Nijmegen
	-1.162	-0.0187	-0.0187	Paris
3S_1	-0.467	0.0581	0.0581	
	-1.082	0.0835	0.0835	
	-1.148	0.0689	0.0689	
	-2.227	0.0208	0.0208	
3S_1 3D_1	0	-0.0017	0.0301	
	0	-0.0034	0.0243	
	0	-0.0039	0.0298	
	0	-0.0047	0.0227	
3D_1	0	-0.0005	-0.0005	
	0	-0.0006	-0.0006	
	0	-0.0005	-0.0005	
	0	-0.0004	-0.0004	

tween $V_{\text{low } k}$ and $P V_{\text{bare}} P + V_{\text{counter}}$; the fit is indeed very good.

As shown in the table, the counter terms are all rather small except for the S waves. This is consistent with the RG-EFT approach where the r -space counter term potential is given as a delta function plus its derivatives [2, 4]. (Delta function has non-zero matrix elements for S waves only.) However, since the C_0 coefficients for the 1S_0 and 3S_1 channels are different, our results indicate that the counter term potential is mainly a spin-dependent delta

TABLE III: Shell model relative matrix elements of $V_{\text{low } k}$ and $(P V_{\text{NN}} P + V_{\text{CT}})$ (column CT), with $\Lambda = 2.0 \text{ fm}^{-1}$ and $\hbar^2 = 19 \text{ MeV}$. Matrix elements are in units of MeV .

TSjnl	n^{0^0}	CDB	CDB-CT	Nij	V18
100 00	00	-9.053	-9.053	-9.066	-9.062
10	00	-6.744	-6.742	-6.698	-6.609
10	20	-3.527	-3.529	-3.363	-3.375
011 00	00	-11.00	-11.00	-10.72	-10.80
02	00	-8.440	-8.405	-8.636	-8.627
02	02	2.450	2.453	2.253	2.263
10	20	-6.873	-6.850	-7.033	-6.738
10	22	-6.969	-6.940	-7.562	-7.637
12	22	2.281	2.278	2.070	2.079
001 01	01	3.835	3.858	3.587	3.670
11	01	3.757	3.781	3.446	3.440
110 01	01	-2.482	-2.452	-2.407	-2.557
11	01	-1.124	-1.099	-0.900	-1.162

force which may be written as

$$V_{\text{CT}} = (f_0 + f_0^0) (\boldsymbol{\sigma} \cdot \boldsymbol{\sigma}); \quad (7)$$

with $f_0 = (3C_0 \langle ^3S_1 \rangle + C_0 \langle ^1S_0 \rangle) = 4$ and $f_0^0 = (C_0 \langle ^3S_1 \rangle + C_0 \langle ^1S_0 \rangle) = 4$. For the coefficients of Table I, we have $f_0 = 0.382 \text{ fm}$ and $f_0^0 = 0.077 \text{ fm}$. It is likely that this spin dependence is closely related to the tensor force in the 3S_1 3D_1 channel. Further study in this direction should be of interest.

Comparing counter term coefficients for different V_{bare} potentials can illustrate key differences between those potentials. Thus, in Table II, we compare the low order counter terms obtained for the CD-Bonn [4], Nijmegen [5], Argonne [6] and Paris [8] NN potentials. The C_0 coefficients for these potentials are significantly different, indicating that one of the chief differences between these potentials is the way in which they treat the short range repulsion. For instance, the Paris potential effectively has a very strong short-range repulsion and consequently its C_0 is much larger compared with the others.

IV. COMPARISON OF SHELL MODEL MATRIX ELEMENTS

In shell model calculations, a basic input is the relative matrix elements $\langle n^0 \text{SJT} | j V_{\text{eff}} | j n^0 \text{SJT} \rangle$, where n^0 and n^0 denote the oscillator wave functions for the relative motion of the two nucleons and S and T are the two-nucleon spin and isospin. The relative momenta l^0 and S couple to total angular momentum J . From these

TABLE IV : A comparison of shell model relative matrix elements calculated using $V_{\text{low } k}$ with those calculated using the Sussex interaction V_{Sussex} . The oscillator length parameter b is given by $b = \sqrt{\frac{\hbar}{m\omega}}$, in units of fm. The matrix elements are in units of MeV. A dash denotes when no Sussex matrix element was available.

	b (fm)	n = 0		n = 1		n = 2		n = 3	
		V_{Sussex}	$V_{\text{low } k}$						
$1n^1S_0 \text{ jV } jn^1S_0 \text{ i}$	1.4	-9.68	-9.96	-4.19	-5.43	-0.93	-1.61	1.37	-2.94
	2.0	-4.85	-4.84	-4.03	-4.40	-2.88	-3.41	-0.47	-2.35
	2.6	-2.68	-2.59	-2.78	-2.80	-2.46	-2.63	-2.06	-2.32
$1n^1S_0 \text{ jV } j(n+1)^1S_0 \text{ i}$	1.4	-7.33	-6.98	-2.82	-3.06	0.05	-2.83	-	-
	2.0	-4.01	-4.48	-3.11	-3.83	-2.11	-2.82	-1.25	-1.81
	2.6	-2.71	-2.64	-2.58	-2.69	-2.21	-2.45	-1.82	-2.13
$1n^1S_0 \text{ jV } j(n+2)^1S_0 \text{ i}$	1.4	-3.55	-4.04	-0.83	-1.05	-	-	-	-
	2.0	-3.14	-3.80	-2.31	-3.13	-1.45	-2.19	-0.71	-1.27
	2.6	-2.48	-2.49	-2.31	-2.49	-1.95	-2.00	-1.58	-1.90
$1n^3S_1 \text{ jV } jn^3S_1 \text{ i}$	1.4	-11.11	-12.29	-5.59	-9.12	-2.02	-4.98	2.20	-1.53
	2.0	-5.58	-5.51	-5.11	-5.70	-3.76	-5.09	-2.53	-4.22
	2.6	-2.68	-2.85	-2.78	-3.32	-2.46	-3.36	-2.06	-3.21
$1n^3S_1 \text{ jV } j(n+1)^3S_1 \text{ i}$	1.4	-6.60	-10.17	-2.41	-6.68	0.21	-2.80	-	-
	2.0	-5.22	-5.45	-4.24	-5.33	-2.93	-4.61	-1.89	-3.71
	2.6	-2.93	-3.02	-3.33	-3.32	-3.10	-3.27	-2.37	-3.01

matrix elements, the two-particle shell model matrix elements in the laboratory frame can be calculated [27]. Thus if $V_{\text{low } k}$ and $P V_{\text{bare}} P + V_{\text{CT}}$ are to prove useful in a broad sense, they must preserve these matrix elements.

In Table III we provide a comparison between these matrix elements as obtained from several input potentials. To begin, we note that the harmonic oscillator matrix elements for $V_{\text{low } k}$ are approximately the same regardless of which of the four bare potentials we use. So, as far as providing input for shell model calculations, this is further evidence that the $V_{\text{low } k}$ is approximately unique. Next, we come to the main result of the table, which is that the matrix elements for $V_{\text{low } k}$ and $V_{\text{bare}} + V_{\text{CT}}$ are in very good agreement. We have used the CD Bonn for the bare potential, but this holds for the other bare potentials as well. In fact for the 1S_0 , 3S_1 , and 3D_1 channels, the elements are virtually exact out to four significant figures, and there is only minimal disagreement in the coupled channel.

Elliott and his coworkers [13] have developed a very interesting method to derive the shell model matrix elements directly from phase shift data. Their matrix elements are commonly referred to as the Sussex interaction. In their method, it is assumed that the effective

interaction is non-singular and that the scattering data below 350 MeV can provide all the necessary information for its determination. This spirit is rather similar to our present $V_{\text{low } k}$ approach, in the sense that a smooth (non-singular) effective interaction for low-energy nuclear properties can be obtained from the low-energy scattering data. It may be of interest to compare their results with our matrix elements.

In Table IV we compare the elements as obtained from $V_{\text{low } k}$ with those obtained from the Sussex interaction. As can be seen from the table, agreement between the two methods is rather sporadic. While not always the case, it appears that agreement is best for larger b and smaller n and tends to get worse as b is decreased and/or n is increased. We can make sense of this trend when we consider that the Sussex method is essentially a distorted-wave Born approximation. Since it is the ratio $\frac{d}{b^2}$ which determines the energy, if we increase n or decrease b , the energy will increase. In the Sussex method, a new auxiliary potential is used for each n value, and thus they take on an energy dependence, making the matrix elements more repulsive at high energies (due to a growing repulsive potential). In addition, the Born approximation used in the Sussex method for phase shift calculations may be

TABLE V : Complete listing of counter terms for all partial waves obtained from the CD-Bonn potential using $\mu = 2\text{fm}^{-1}$. The units for the counter coefficients are the same as in Table I.

Wave	C_0	C_2	C_2^0	C_4	C_4^0	C_6	C_6^0	C_6^{00}
1S_0	-0.1580	-1.309E-2	-1.309E-2	3.561E-4	-8.469E-4	-5.795E-6	-1.191E-4	-1.191E-4
3S_1	-0.4646	5.815E-2	5.815E-2	-1.539E-3	-1.135E-2	-3.613E-4	4.832E-4	4.832E-4
3S_1 3D_1	0.0	-1.750E-3	3.006E-2	-1.338E-3	-4.666E-3	6.209E-4	-1.339E-4	-3.393E-4
3D_1	0.0	-5.344E-4	-5.344E-4	5.667E-4	-1.796E-3	-1.247E-4	-1.041E-4	-1.041E-4
1P_1	0.0	-2.132E-2	-2.132E-2	1.235E-2	-2.621E-2	-2.216E-3	2.258E-3	2.258E-3
3P_0	0.0	-2.613E-2	-2.613E-2	1.417E-2	-3.142E-2	-2.385E-3	2.883E-3	2.883E-3
3P_1	0.0	-2.671E-2	-2.671E-2	1.520E-2	-3.271E-2	-2.681E-3	2.875E-3	2.875E-3
3P_2	0.0	-6.993E-3	-6.993E-3	4.525E-3	-6.133E-3	-8.409E-4	5.618E-4	5.618E-4
3P_2 3F_2	0.0	8.667E-5	9.005E-5	-9.397E-5	-6.446E-5	2.138E-5	3.014E-5	-1.696E-6
3F_2	0.0	-2.832E-6	-2.833E-6	2.902E-7	9.258E-6	3.604E-7	-9.656E-6	-9.658E-6
1D_2	0.0	-2.698E-4	-2.698E-4	2.981E-4	-4.916E-4	-6.686E-5	-2.385E-5	-2.385E-5
3D_2	0.0	-1.732E-3	-1.732E-3	1.925E-3	-1.328E-3	-4.312E-4	-2.655E-4	-2.655E-4
3D_3	0.0	-9.635E-4	-9.635E-4	8.178E-4	-5.714E-3	-1.608E-4	5.201E-4	5.201E-4
3D_3 3F_3	0.0	-4.692E-5	-2.971E-5	-2.627E-5	3.255E-4	1.269E-5	4.098E-5	-9.052E-5
3F_3	0.0	-9.111E-5	-9.111E-5	5.549E-5	1.833E-4	-8.251E-6	-4.472E-5	-4.472E-5
1F_3	0.0	-1.736E-5	-1.739E-5	3.334E-5	-1.252E-5	-7.710E-6	-4.069E-5	-4.059E-5
3F_3	0.0	-1.080E-5	-1.079E-5	8.650E-6	1.702E-5	-1.499E-6	-9.250E-6	-9.252E-6
3F_4	0.0	2.125E-6	2.051E-6	8.764E-6	-8.884E-5	-1.994E-6	-4.208E-6	-3.961E-6
3F_4 3H_4	0.0	1.134E-5	8.240E-6	-8.824E-6	-1.154E-5	1.744E-6	8.103E-6	5.415E-7
3H_4	0.0	-4.128E-6	-4.183E-6	2.358E-6	8.487E-6	-3.245E-7	-1.903E-6	-1.919E-6
1G_4	0.0	-4.720E-6	-4.723E-6	2.993E-6	1.111E-5	-4.312E-7	-3.630E-6	-3.645E-6
3G_4	0.0	-1.173E-4	-1.173E-4	7.747E-5	2.511E-4	-1.195E-5	-7.500E-5	-7.500E-5
3G_5	0.0	5.439E-5	5.440E-5	-3.791E-5	-7.620E-5	7.832E-6	-1.827E-5	-1.827E-5
3G_5 3H_5	0.0	8.678E-6	3.654E-6	-4.765E-6	-1.551E-5	8.103E-7	1.053E-5	9.246E-7
3H_5	0.0	-1.268E-5	-1.272E-5	7.103E-6	2.593E-5	-9.867E-7	-5.486E-6	-5.500E-6
1H_5	0.0	-5.571E-6	-5.311E-6	2.784E-6	1.186E-5	-2.409E-7	-2.872E-6	-3.757E-6
3H_5	0.0	-3.482E-6	-3.482E-6	1.772E-6	1.210E-5	-4.270E-7	-2.354E-6	-2.354E-6
3H_6	0.0	1.047E-7	1.047E-7	1.095E-7	6.252E-6	-9.967E-8	-2.078E-6	-2.078E-6
3H_6 3I_6	0.0	-7.129E-9	-6.670E-9	-3.676E-8	1.991E-6	-1.086E-7	-3.574E-8	-3.863E-8
3I_6	0.0	0.0	0.0	0.0	-8.368E-7	0.0	0.0	0.0

less accurate at high energies. These considerations are likely the reason for the main differences seen in the table. It is remarkable that the Sussex and $V_{\text{low } k}$ matrix elements are very close to each other for the $n=0$ cases.

V. CONCLUSION

While there are several models for the nucleon-nucleon potential in use today, they suffer from uncertainty and model dependence. Motivated by RG-EFT ideas, a low momentum NN interaction, $V_{\text{low } k}$, has been constructed via integrating out the high momentum, model dependent components of these different potentials. The result

appears to give an approximately unique representation of the low momentum NN potential, and the main issue addressed in this paper was whether or not this $V_{\text{low } k}$ could accurately be cast in some algebraic form. We have shown that this was indeed the case as $V_{\text{low } k}$ is nearly identical to $V_{\text{NN}} + V_{\text{CT}}$ over all partial waves, and that $V_{\text{NN}} + V_{\text{CT}}$ reproduces both the deuteron binding energy and the NN phase shifts in the low momentum region. Our results suggest that the counter term potential is mainly a spin dependent delta interaction, namely $V_{\text{CT}} = (f_0 + f_0^0) (\hat{t})$.

We have further examined the potential for using $V_{\text{low } k}$ and $V_{\text{NN}} + V_{\text{CT}}$ in shell model calculations. Again, it was seen that not only does $V_{\text{low } k}$ give ap-

proximately identical input matrix elements irrespective of which bare potential was used, but that the counter term approach provided nearly the same results. Thus we have shown that the high momentum information integrated out of each bare NN potential can be accurately replaced by the counter terms, making the use of $V_{low k}$ in a broad context much more tractable.

Acknowledgments

Many helpful discussions with Ruprecht Machleidt and Achim Schwenk are gratefully acknowledged. This work was supported in part by the U.S. DOE Grant No. DE-FG 02-88ER 40388.

-
- [1] S. Weinberg, Phys. Lett. B 251, 288 (1990); Nucl. Phys. B 363, 3 (1991).
- [2] P. Lepage, "How to Renormalize the Schroedinger Equation" in Nuclear Physics (ed. by C.A. Bertulani et al), p.135 World Scientific Press (1997), nucl-th/9706029.
- [3] D.B. Kaplan, M.J. Savage and M.B. Wise, Phys. Lett. B 424, 390 (1998); Nucl. Phys. B 534, 329 (1998), nucl-th/9802075.
- [4] E. Epelbaum, W. Glockle, A. Kugler and Ulf G. Meissner, Nucl. Phys. A 645, 413 (1999).
- [5] P. Bedaque et. al. (eds.), Nuclear Physics with Effective Field Theory II, (1999) World Scientific Press.
- [6] U. van Kolck, Prog. Part. Nucl. Phys. 43, 409 (1999).
- [7] W. Haxton and C.L. Song, Phys. Rev. Lett. 84, 5484 (2000), nucl-th/9907097.
- [8] S. Bogner, T.T.S. Kuo and L. Coraggio, Nucl. Phys. A 684, 432c (2001), nucl-th/0204058.
- [9] S. Bogner, T.T.S. Kuo, L. Coraggio, A. Covello and N. Itaco, Phys. Rev. C 65, 051301(R) (2002), nucl-th/9912056.
- [10] T.T.S. Kuo, S. Bogner and L. Coraggio, Nucl. Phys. A 704, 107c (2002).
- [11] A. Schwenk, G.E. Brown and B. Friman, Nucl. Phys. A 703, 745 (2002), nucl-th/0109059.
- [12] L. Coraggio, A. Covello, A. Gargano, N. Itako, T.T.S. Kuo, D.R. Entem and R. Machleidt, Phys. Rev. C 66, 021303(R) (2002), nucl-th/0206025.
- [13] J.P. Elliott, A.D. Jackson, H.A. Mavromatis, E.A. Sanderson and B. Singh, Nucl. Phys. A 121, 241 (1968).
- [14] R. Machleidt, Phys. Rev. C 63, 024001 (2001), nucl-th/0006014.
- [15] V.G.J. Stoks and R. Klop, C. Terheggen and J. de Schwart, Phys. Rev. C 49, 2950 (1994), nucl-th/9406039.
- [16] R.B. Wiringa, V.G.J. Stoks and R. Schiavilla, Phys. Rev. C 51, 38 (1995), nucl-th/9408016.
- [17] D.R. Entem, R. Machleidt and H. Witala, Phys. Rev. C 65, 064005 (2002), nucl-th/0111033.
- [18] M. Lacombe et al., Phys. Rev. C 21, 861 (1980).
- [19] T.T.S. Kuo, S.Y. Lee and K.F. Ratcli, Nucl. Phys. A 176, 65 (1971).
- [20] T.T.S. Kuo and E. Osnes, Springer Lecture Notes of Physics, Vol. 364, p.1 (1990).
- [21] K. Suzuki and S.Y. Lee, Prog. Theor. Phys. 64, 2091 (1980).
- [22] F. Andreozzi, Phys. Rev. C 54, 684 (1996).
- [23] E.M. Krenciglowa and T.T.S. Kuo, Nucl. Phys. A 235, 171 (1974).
- [24] S. Okubo, Prog. Theor. Phys. 12, 603 (1954).
- [25] K. Suzuki and R. Okamoto, Prog. Theo. Phys. 70, 439 (1983).
- [26] T.T.S. Kuo, P.J. Ellis, Jifa Hao, Zibang Li, K. Suzuki, R. Okamoto and H. Kumagai, Nucl. Phys. A 560, 622 (1993).
- [27] T.T.S. Kuo and G.E. Brown, Nucl. Phys. 85, 40 (1966).